AIP Applied Physics Letters

Fundamental piezoresistive coefficients of p-type single crystalline 3C-SiC

Hoang-Phuong Phan, Dzung Viet Dao, Philip Tanner, Li Wang, Nam-Trung Nguyen, Yong Zhu, and Sima Dimitrijev

Citation: Applied Physics Letters **104**, 111905 (2014); doi: 10.1063/1.4869151
View online: http://dx.doi.org/10.1063/1.4869151
View Table of Contents: http://scitation.aip.org/content/aip/journal/apl/104/11?ver=pdfcov
Published by the AIP Publishing

Fundamental piezoresistive coefficients of p-type single crystalline 3C-SiC

Hoang-Phuong Phan,[1,a)] Dzung Viet Dao,[1,2] Philip Tanner,[1] Li Wang,[1] Nam-Trung Nguyen,[1] Yong Zhu,[1,2] and Sima Dimitrijev[1,2]
[1]*Queensland Micro- and Nanotechnology Centre, Griffith University, Queensland, Australia*
[2]*School of Engineering, Griffith University, Queensland, Australia*

(Received 29 January 2014; accepted 10 March 2014; published online 19 March 2014)

The orientation dependence of the piezoresistive effect of p-type single crystalline 3C-SiC thin film grown on a (100)Si wafer was characterized. The longitudinal, transverse gauge factors in [100] orientation, and longitudinal gauge factor in [110] orientation were found to be 5.8, −5.2, and 30.3, respectively. The fundamental piezoresistive coefficients π_{11}, π_{12}, and π_{44} of p-type 3C-SiC were obtained to be $1.5 \times 10^{-11}\,\mathrm{Pa}^{-1}$, $-1.4 \times 10^{-11}\,\mathrm{Pa}^{-1}$, and $18.1 \times 10^{-11}\,\mathrm{Pa}^{-1}$, respectively. From these coefficients, the piezoresistive effect in any crystallographic orientation in p-type single crystalline 3C-SiC can be estimated, which is very valuable in designing micro-mechanical sensors. © *2014 AIP Publishing LLC*. [http://dx.doi.org/10.1063/1.4869151]

Silicon carbide (SiC) is a promising material for MEMS (Micro Electro Mechanical Systems) transducers used in harsh environments, due to its high energy band gap, chemical inertness, and high stiffness.[1] Among many poly types, the cubic crystal silicon carbide (3C-SiC) is considered to be the most suitable polytype for MEMS applications, since it can be grown directly on a Si substrate and the electrical insulation between 3C-SiC layer and Si substrate is achieved by the SiC/Si heterojunction.[2]

One of the most common methods for mechanical sensing is based on the piezoresistive effect which has been intensively studied in Si so far.[3–5] Research on the piezoresistive effect of 3C-SiC recently attracted significant attention for applications used in high temperature environments.[6–10] Large piezoresistive effects in n-type single crystalline 3C-SiC with the longitudinal gauge factors (GF) as large as −31.8 in [100] orientation have been reported.[9,10] Various piezoresistive pressure sensors based on n-type 3C-SiC with the large range of operating temperature up to 500 °C have been developed, demonstrating the high potential of 3C-SiC material in MEMS sensing devices.[11–13] Most previous studies presented the piezoresistive effect in n-type 3C-SiC, with very limited results being available for p-type 3C-SiC.[14] One considerable reason for the limited work on p-type 3C-SiC is due to the high growth temperature at around 1350 °C which causes the redistribution of the dopant in Si and the accumulation of the thermal mismatch between SiC and Si.[18] In a previous study,[2] we have characterized the piezoresistive effect in [110] orientation of p-type single crystalline 3C-SiC thin film grown on a Si substrate by LPCVD (Low Pressure Chemical Vapor Deposition) at low temperature of 1000 °C with large GF of 30.3.

Understanding of the piezoresistive effect in arbitrary crystallographic orientations plays an important role in designing highly sensitive p-type single crystalline 3C-SiC based mechanical sensors. Therefore, the aim of this paper is to determine the fundamental piezoresistive coefficients, and to investigate the orientation dependence of the piezoresistive effect in p-type single crystalline 3C-SiC.

a)Electronic mail: hoangphuong.phan@griffithuni.edu.au

The p-type single crystalline 3C-SiC with the thickness of 280 nm was epitaxially grown on p-type (100) Si, and *in-situ* doped with aluminum by using LPCVD.[19] The full-range $2\theta - \omega$ of the X-Ray Diffraction (XRD) measurement indicated that single crystalline (100)3C-SiC was grown on Si substrate (Fig. 1(a)). The full width at half maximum (FWHM) of SiC(200) peak in the $2\theta - \omega$ scan is 0.26°. The FWHM of rocking curve scan of the SiC(200) peak is 0.80° as shown in Fig. 1(b). The transmission electron microscopy (TEM) image in Fig. 1(c) shows that there are no boundaries in the single crystalline 3C-SiC and the only defects are stacking faults. The selected area electron diffraction (SAED) displayed in Fig. 1(d) confirms that the grown 3C-SiC is single crystalline. The Hall-effect measurement was performed to characterize the electrical properties of the grown SiC film. The resistivity of the SiC film was measured to be 0.14 Ω cm and the hole mobility of the single crystalline 3C-SiC film

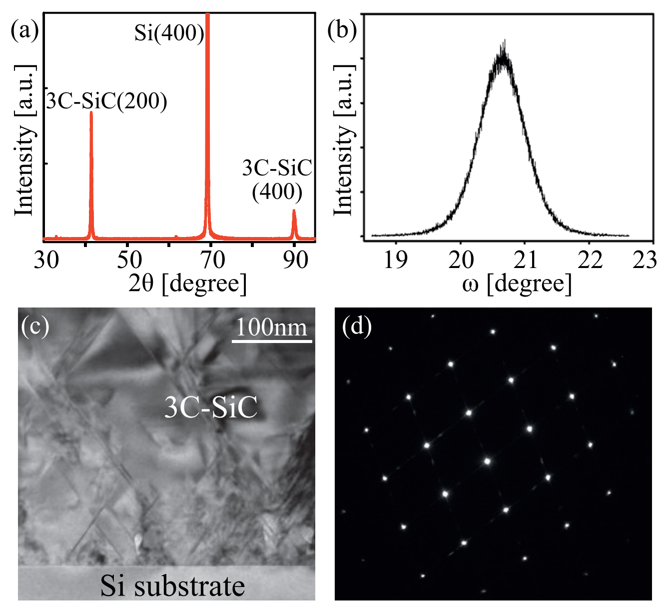

FIG. 1. (a) The XRD graph of 3C-SiC grown on (100)Si; (b) The rocking curve scan of 3C-SiC; (c) The TEM image of 3C-SiC; (d) The SAED image of 3C-SiC.

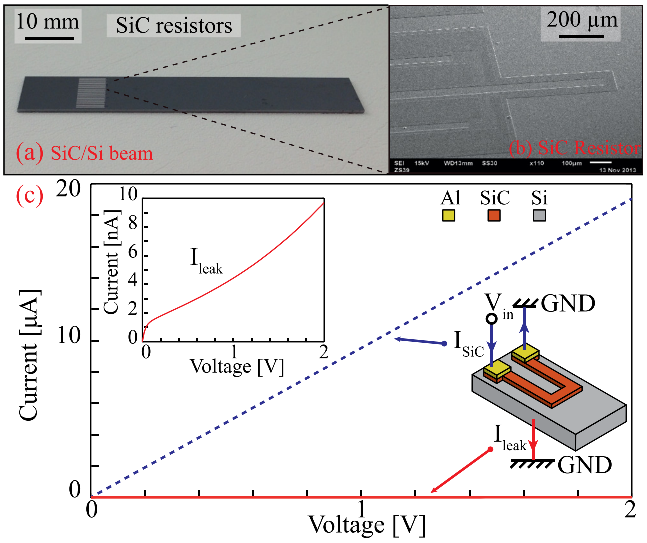

FIG. 2. (a) Photograph of the SiC/Si beam; (b) SEM image of a SiC resistor; (c) IV curve of SiC resistor (small graph: zoom-in of the current leakage through SiC/Si junction).

was found to be 9 cm^2/Vs which is a reasonable value for the doping level of $5 \times 10^{18}\,cm^{-3}$, indicating the good crystal quality. SiC piezoresistor on Si substrate was patterned by a conventional photolithography process and then diced into a strip 60 mm × 9 mm × 0.625 mm (Fig. 2(a)). Scanning electron microscopy (SEM) photograph of a SiC resistor is shown in Fig. 2(b). The carrier concentration of the p-type single crystalline SiC in this research was $5 \times 10^{18}\,cm^{-3}$, while the carrier concentration of the Si substrate was $5 \times 10^{14}\,cm^{-3}$. The issue of current leakage through SiC and Si junction was investigated to make sure that Si would not affect the measured gauge factor of SiC. The current leakage through SiC/Si heterojunction at the applied voltage of 0.5 V was found to be about 0.05% of the current flowing through SiC resistor as shown in Fig. 2(c). This result indicates that Si substrate will not contribute to the measurement of the GF of the SiC thin film.

The GF is measured by the bending beam method, and the four point measurement was employed to determine the resistance change of the p-type 3C-SiC (Fig. 3). GFs of the SiC resistors were obtained from the relative resistance change and the strain: $GF = (\Delta R/R)/\varepsilon_{SiC}$. In order to calculate the strain ε_{SiC} of the SiC layer, bending model of a bilayered beam was taken into account as the SiC was epitaxially grown on Si substrate. The lateral strain of SiC resistance is[20]

$$\varepsilon_{SiC}(x) = -\frac{F}{wD_1}(L_1 + L_2 - x)t_n, \tag{1}$$

where F is the applied force; t_n is the distance from neutral axis to the SiC layer; and parameters w, L_1, L_2 are dimensions as described in Fig. 3(a). The bending modulus per unit width D_1 is deduced from[21]

$$D_1 = \frac{E_1^2 t_1^4 + E_2^2 t_2^4 + 2E_1E_2t_1t_2(2t_2^2 + 2t_1^2 + 3t_1t_2)}{12(E_1t_1 + E_2t_2)}, \tag{2}$$

where E_1 is the Young's modulus of SiC (330 GPa),[22] and E_2 is the Young's modulus of Si (130 GPa in [100] orientation and 169 GPa in [110] orientation). As the thickness of SiC in our design is only 0.05% of the Si layer, the strain calculated from Eq. (1) is approximately the same as that of the upper surface of the Si substrate.[2] Finite Element Method (FEM) was carried out, using COMSOL multiphysics to estimate the strain of the beam. The simulation result was in agreement with the theoretically calculated value discussed above. Accordingly, the strains of the SiC resistors were in the ranges of 0 ∼ 820 ppm and 0 ∼ 1100 ppm for resistors aligned in [110] orientation and [100] orientation, respectively. From the possible errors of the SiC/Si beam dimensions and the misalignment of SiC resistor on Si beam occurred during fabrication process,[23] we estimated the error of the strain obtained from the simulation is about 5%. Figure 4 shows the relationship between relative resistance change and applied strain, which reveals that SiC resistor in [110] direction is more sensitive than that aligned in [100] direction. The longitudinal GFs in [100] and [110] orientation have a positive value of +5.0 and +30.3, respectively, while the transverse GF in [100] orientation has a negative value of −4.6.

Table I shows the comparison between the GF of p-type 3C-SiC presented in this work with the GFs of other polytypes reported in the literature. The GF of n-type 3C-SiC

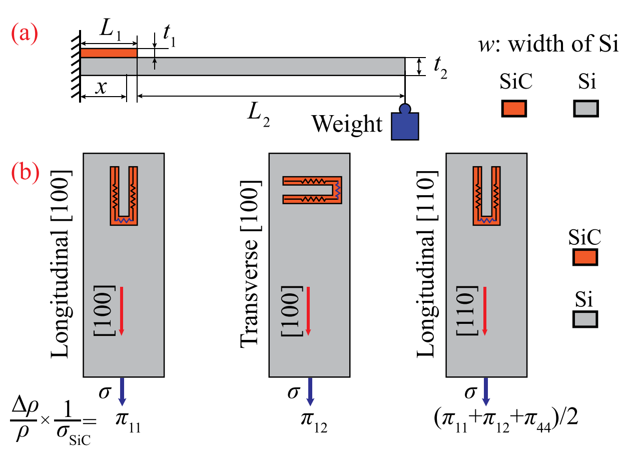

FIG. 3. Schematic diagram showing the bending experiment for measuring the gauge factors: (a) side view; (b) top view of cantilever.

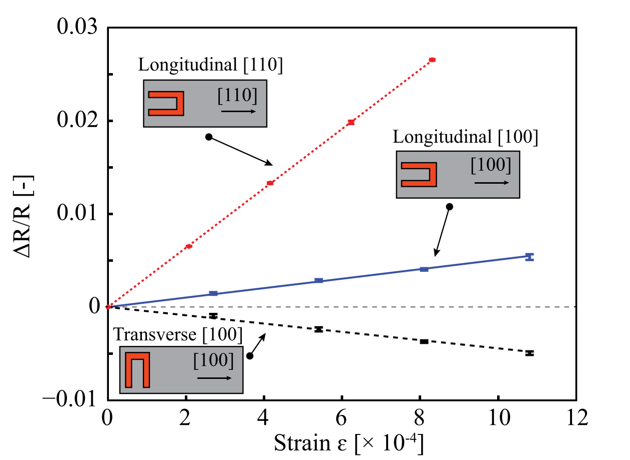

FIG. 4. Relationship between relative resistance change of SiC resistors aligned in different orientations and applied strains.

TABLE I. List of GF of single crystalline SiC in this work and the literature. (* indicated the result in this study)

Polytype	Growing process	Type	Carriers concentration	Thickness of SiC (μm)	GF
3C-SiC*	LPCVD	p	5×10^{18}	0.28	30.3
3C-SiC (Ref. 10)	APCVD[a]	n	$\sim 10^{18}$	10	−31.8
3C-SiC (Ref. 9)	HMCVD[b]	n	$\sim 10^{18}$	2	−27
3C-SiC (Ref. 13)	APCVD	n	unintentional	0.5	−18.8
3C-SiC (Ref. 7)	LPCVD	n	$0.4 \sim 2 \times 10^{17}$	2.3	−24.8
				0.2	3
4H-SiC (Ref. 15)	…	n	1.5×10^{19}	1	20.8
6H-SiC (Ref. 16)	…	n	3.8×10^{18}	2	−29.4
6H-SiC (Ref. 17)	…	p	2×10^{19}	2	27

[a]Atmospheric Pressure Chemical Vapor Deposition (APCVD).
[b]Hot Mesh Chemical Vapor Deposition (HMCVD).

varies with the growth conditions, the thickness of the SiC and the doping level. The results found in this study are quite impressive as the GF of p-type single crystalline 3C-SiC thin film (280 nm) is comparable with previous research in n-type 3C-SiC with larger thicknesses.

The GFs measured above were used to calculate the fundamental piezoresistive coefficients. The change of the resistivity of SiC is[24]

$$\Delta\rho/\rho = GF \times \varepsilon = \pi_l\sigma_l + \pi_t\sigma_t + \pi_s\sigma_s, \tag{3}$$

where σ_l, σ_t, σ_s are longitudinal, transverse, and shear stresses, respectively, and π_l, π_t, π_s are longitudinal, transverse, and shear piezoresistive coefficients, respectively. Let θ be the angle between longitudinal axis of the SiC resistor and [100] orientation in (100) plane. π_l, π_t, π_s are deduced from the fundamental piezoresistive coefficients as[24]

$$\begin{cases} \pi_l = \pi_{11} - \dfrac{1}{2}(\pi_{11} - \pi_{12} - \pi_{44})\sin^2 2\theta \\ \pi_t = \pi_{12} + \dfrac{1}{2}(\pi_{11} - \pi_{12} - \pi_{44})\sin^2 2\theta \, . \\ \pi_s = -\dfrac{1}{2}(\pi_{11} - \pi_{12} - \pi_{44})\sin 4\theta \end{cases} \tag{4}$$

From Eqs. (3) and (4), and the GFs measured in [100] ($\theta = 0°$) and [110] ($\theta = 45°$) orientations, the fundamental piezoresistive coefficient in the principal coordinate π_{11}, π_{12} and π_{44} were found to be $1.5 \times 10^{-11}\,\mathrm{Pa}^{-1}$, $-1.4 \times 10^{-11}\,\mathrm{Pa}^{-1}$, $18.1 \times 10^{-11}\,\mathrm{Pa}^{-1}$, respectively. This result indicates that the piezoresistive effect in p-type single crystalline 3C-SiC has the same characteristic as p-type single crystalline Si, i.e., the shear piezoresistive coefficient (π_{44}) is much larger than normal piezoresistive coefficients (π_{11} and π_{12}). As 3C-SiC has the cubic crystal structure like Si, the model of effect of strain and symmetry in cubic semiconductor proposed by Bir and Pikus[25] can be used to explain the piezoresistive effect in single crystalline 3C-SiC. The piezoresistive coefficients π_{11}, π_{12} are corresponding to the uniaxial stresses applied in [100] direction in which the band warping is negligible, and the dominant mechanism of the piezoresistance is the change of scattering rate which is relatively small. The piezoresistive coefficients π_{44} on the other hand, is corresponding to the uniaxial stress in [110] orientation, where the energy surface is significantly warped, leading to the change of the effective mass and hole occupation in the heavy hole and light hole bands. Therefore, the uniaxial stress in [110] orientation is considered to bring more significant piezoresistive effect than the uniaxial stress in [100] orientation.

Based on the fundamental piezoresistive coefficients, the piezoresistive effect in an arbitrary crystallographic orientation can be estimated, which plays an important role in designing the sensitivity of p-type single crystalline 3C-SiC based mechanical sensors. The longitudinal, transverse, and shear piezoresistive coefficients of an arbitrary orientation in (100)SiC plane is graphically presented in Fig. 5. It can be seen that in [110] orientation, the transverse and longitudinal coefficients reach maximum values.

In conclusion, the fundamental piezoresistive coefficients of p-type single crystalline 3C-SiC were obtained. The gauge factor of p-type 3C-SiC resistor is significantly dominated by the shear piezoresistive coefficient π_{44}. Compared to p-type single crystalline silicon[24] ($\pi_{44} = 115 \times 10^{-11}\,\mathrm{Pa}^{-1}$ at the doping concentration of $5 \times 10^{18}\,\mathrm{cm}^{-3}$), the shear piezoresistive coefficient of p-type single crystalline SiC is relatively small. However, with the advantages of 3C-SiC such as wide bandgap, high melting point, high Q factor, and excellent chemical inertness, the piezoresistive effect in p-type single

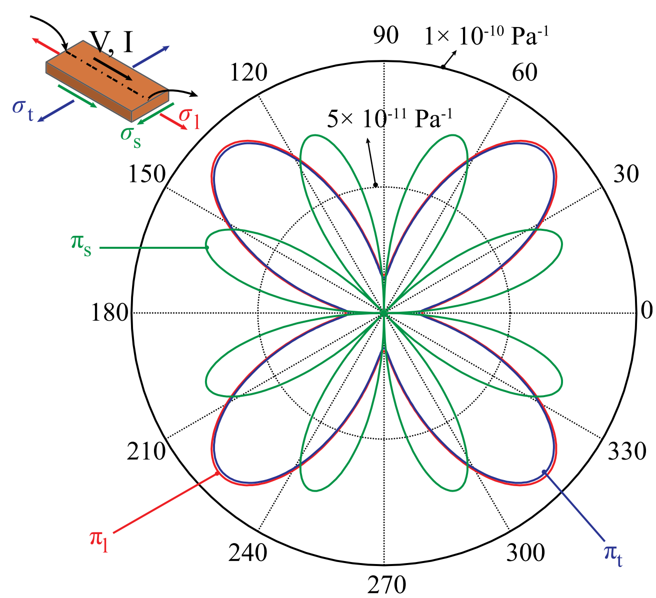

FIG. 5. Piezoresistive coefficients π_l, π_t, π_s in (100) plane of p-type single crystalline 3C-SiC (In some literature,[24] π_l, π_t, π_s are denoted as π'_{11}, π'_{12} and π'_{16}).

crystalline 3C-SiC is a potential candidate for harsh environment and high frequency applications. From graphical study on the dependence of the piezoresistive coefficients on orientation, we suggest that when designing p-type 3C-SiC based mechanical sensors in the (100) plane, the [110] orientation should be selected to achieve maximum sensitivity.

The authors would like to thank Dr. Jisheng Han, Lin Zhang at Queensland Micro- and Nanotechnology Centre, and Harrison Brooke at Griffith University for the preparation of the samples. This work was performed in part at the Queensland node of the Australian National Fabrication Facility, a company established under the National Collaborative Research Infrastructure Strategy to provide nano and micro-fabrication facilities for Australia's researchers. This work has been partially supported by the Griffith University's New Researcher Grants.

[1]M. Mehregany, C. A. Zorman, N. Rajan, and C. H. Wu, Proc. IEEE **86**(8), 1594 (1998).
[2]H. P. Phan, P. Tanner, D. V. Dao, L. Wang, N. T. Nguyen, Y. Zhu, and S. Dimitrijev, IEEE Electron Device Lett. **35**(3), 399–401 (2014).
[3]D. V. Dao, T. Toriyama, J. Wells, and S. Sugiyama, Sens. Mater. **15**(3), 113 (2003).
[4]D. V. Dao, T. Toriyama, and S. Sugiyama, in *Proceedings of IEEE Sensors 2004, Vienna, Austria* (IEEE, 2004), p. 1464.
[5]D. V. Dao, K. Nakamura, T. T. Bui, and S. Sugiyama, Adv. Nat. Sci: Nanosci. Nanotechnol. **1**(1), 013001 (2010).
[6]J. Bi, G. Wei, L. Wang, F. Gao, J. Zheng, B. Tang, and W. Yang, J. Mater. Chem. C. **1**, 4514 (2013).
[7]M. Eickoff, M. Moller, G. Kroetz, and M. Stutzmann, J. Appl. Phys. **96**, 2872 (2004).
[8]T. Toriyama and S. Sugiyama, Appl. Phys. Lett. **81**, 2797 (2002).
[9]K. Yasui, H. Miura, M. Takata, and T. Akahane, Thin Solid Films **516**, 644 (2008).
[10]S. J. Shor, D. Goldstein, and A. D. Kurtz, IEEE Trans. Electron Devices. **40**(6), 1093 (1993).
[11]R. Ziermann, J. von Berg, E. Obermeier, F. Wischmeyer, E. Niemann, H. Moller, M. Eickhoff, and G. Krotz, Mater. Sci. Eng. B **61–62**, 576 (1999).
[12]G. H. Kroetz, M. H. Eickhoff, and H. Moeller, Sens. Actuators A **74**, 182 (1999).
[13]C. H. Wu, C. A. Zorman, and M. Mehregany, IEEE Sensors. J. **6**(2), 316 (2006).
[14]T. Homma, K. Kamimura, H. Y. Cai, and Y. Onuma, Sens. Actuators A **40**(2), 93 (1994).
[15]T. Akiyama, D. Briand, and N. F. Rooij, J. Micromech. Microeng. **22**, 085034 (2012).
[16]J. S. Shor, L. Bemis, and A. D. Kurtz, IEEE Trans. Electron Devices **41**(5), 661 (1994).
[17]R. S. Okojie, A. A. Ned, A. D. Kurtz, and W. N. Carr, IEEE Trans. Electron Devices **45**(4), 785 (1998).
[18]L. Wang, S. Dimitrijev, J. S. Han, P. Tanner, A. Iacopi, and L. Hold, J. Cryst. Growth. **329**, 67 (2011).
[19]L. Wang, S. Dimitrijev, G. Walker, J. S. Han, A. Iacopi, P. Tanner, L. Hold, Y. Zhao, and F. Iacopi, Mater. Sci. Forum **740–742**, 279–282 (2013).
[20]X. Gao, W. H. Shih, and W. Y. Shih, Smart Mater. Struct. **18**, 125018 (2009).
[21]X. Li, W. Y. Shih, I. A. Aksay, and W. H. Shih, J. Am. Ceram. Soc. **82**(7), 1733 (1999).
[22]F. Iacopi, G. Walker, L. Wang, L. Malesys, S. Ma, B. V. Cunning, and A. Iacopi, Appl. Phys. Lett. **102**, 011908 (2013).
[23]See supplementary material at http://dx.doi.org/10.1063/1.4869151 for the estimation of the different between the simulation and the actual results of the strain in SiC resistor.
[24]Y. Kanda, Sens. Actuators, A **28**, 83 (1991).
[25]Y. Sun, S. E. Thompson, and T. Nishida, *Strain Effect in Semiconductor: Theory and Device Applications*, 1st ed. (Springer, 2009).